Effects of Perfusion on Cardiac MR Diffusion Measurements

Osama Abdullah[1], Arnold David Gomez[1], Samer Merchant[1], Owen Stedham[1], Michael Heidinger[2], Steven Poelzing[2], and Edward Hsu[1]
[1]*Bioengineering, University of Utah, salt lake city, Utah, United States,* [2]*Cardiovascular Research and Training Institute, University of Utah, salt lake, Utah, United States*

Introduction Diffusion tensor imaging (DTI) (1) has become a preferred technique for characterizing the cardiac myofiber structure (2). Despite challenges presented by bulk motion and strain memory effects, *in vivo* cardiac DTI has been shown feasible [3, 4]. According to the intravoxel incoherent motion (IVIM) theory [5], the observed apparent diffusion coefficient (ADC) is known to depend on tissue perfusion and the measurement methodology (e.g., b-values used). However, the precise effects of perfusion on *in vivo* cardiac DTI remain largely unknown. Of particular concern is that, due to hardware constraint or to alleviate motion artifacts, *in vivo* cardiac DTI is often performed using low or moderate b-values where the dependence on perfusion is the most pronounced. Using an animal model of isolated perfused heart to precisely control myocardial perfusion, the goals of this work are to empirically investigate the effects of perfusion on cardiac diffusion measurements and to assess their implications for *in vivo* cardiac DTI.

Methods Guinea pig hearts (n=8) were rapidly excised and attached to a MR-compatible Langendorff system, perfused and arrested with Tyrode solution and potassium (20 mM) at ~36 °C as described previously (6). The heart was placed along a sealed-tube water phantom inside a loop-gap resonator and scanned using a Bruker Biospec (7T) instrument under two perfusion settings: normal (aortic pressure 52 mmHg) and low (16 mmHg). The heart was allowed to beat for ~10 min between flow settings to ascertain its viability post-hyperkalemia. At each flow setting, regional tissue perfusion and ADC were quantified on a 3 mm short-axis slice via flow-sensitive-inversion-recovery single-shot EPI-SE sequence (10 s TR, 35 ms TE, 300 μm in-plane resolution, and 22 inversion times from 30 ms to 10 sec) and diffusion weighted 4-shot EPI-SE sequence (2 s TR, 25 ms TE, 5 ms δ, 11 ms Δ, and 235 μm in-plane resolution), respectively. Diffusion scans were encoded in both slice and readout directions with 13 b-values ranging from 1 to 1000 s/mm^2. Parallel and perpendicular ADCs, namely $ADC_{//}$ and $ADC_{\perp}$, were quantified over the full b-value range in the mid left-ventricular circumferential fibers where the myofibers run mostly parallel and perpendicular to the read and slice directions, respectively. To examine the dependency of perfusion effects on the choice of b-values, ADCs were also quantified with either only the lower b-values (b < 100 s/mm^2) or higher b-values (b ≥ 160 s/mm^2), to enhance or reduce sensitivity to possible perfusion effects (7). Averaged ADC values were normalized to reference water phantom and compared via paired t-tests. All entries are reported as mean ± SEM.

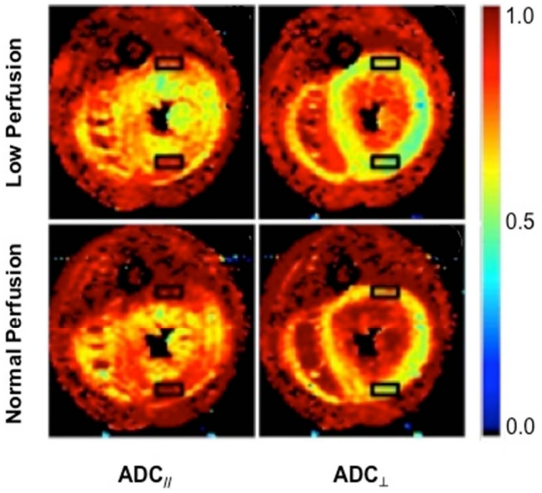

Figure 1. Normalized diffusion maps at low (top row) and normal (lower row) flow conditions. Diffusion encoding was applied in readout (left column), and perpendicular directions (right column). Black boxes represent the locations of the averaged ROIs used in Table 1, where the myofibers run parallel and perpendicular to the read and slice directions, respectively.

Table 1. Normalized $ADC_{//}$ and $ADC_{\perp}$ at normal and low flow conditions when estimated using full b range, low-only and high-only b-values. The parentheses indicate percent change of normal from low flow ADC values, with asterisks denoting statistically significant differences (P < 0.05).

	$ADC_{//}$		$ADC_{\perp}$	
b-value	Normal Flow	Low Flow	Normal Flow	Low Flow
Full range	0.84±0.04 (14%*)	0.74±0.05	0.54±0.03 (10%*)	0.49±0.03
Low b only	1.01±0.06 (22%*)	0.83±0.06	0.73±0.04 (28%*)	0.57±0.03
High b only	0.77±0.04 (10%)	0.70±0.05	0.49±0.03 (9%)	0.45±0.02

Results and Discussion The flow conditions were verified by direct perfusion measurements, which reported 13 ± 6 and 89 ± 10 ml/(100g min) for the low and normal flow settings, respectively. Figure 1 shows the normalized ADC maps obtained for a representative heart. The tabulated ADC values (Table 1) indicate that the presence of flow leads to significantly increased $ADC_{//}$ and $ADC_{\perp}$ (14% and 10%, respectively) when observed over the full b-value range. Based on the axisymmetric diffusion tensor model (8), the ADC differences correspond to a 7%, albeit insignificant (P = 0.48), increase in the FA. Table 1 also shows that perfusion effects were accentuated when ADCs were obtained using only low b-values, but the effects were reduced when only higher b-values were used exclusively. The above observations are consistent in general with IVIM studies performed in organs such as the liver (9) and muscle (10), albeit the dependence of $ADC_{\perp}$ on perfusion has not been predicted (10,11). Findings of the current study suggest that, depending on the b-values used, *in vivo* cardiac DTI may yield scalar diffusivity measurements, including eigenvalues, mean diffusivity, trace, and possibly FA, that contain significant effects of myocardial perfusion. Because myocardial perfusion in turn is dependent on other factors such as the cardiac cycle, appropriate caution in taking the underlying physiology into account is warranted when interpreting *in vivo* cardiac DWI or DTI results.

References [1] Basser et al, Biophs J 1994; 66:254-267. [2] Hsu et al, AJPHCP 1998; 275:H2308–18. [3] Dou et al, MRM 2002 48:105–14. [4] Gamper et al, MRM 2007; 57:331–7. [5] Le Bihan et al, Radiology 1986; 161:401–407. [6] Veeraraghavan et al, AJPHCP 2012; 302: H278–H286. [7] Le Bihan et al, Radiology 1988;168:497-505. [8] Hsu et al, MRM 1995;34(2):194-200. [9] Yamada et al, Radiology 1999; 210:617–23. [10] Karampinos et al, JMRI 2010; 31:942–53. [11] Callot et al, MRM 2003; 50:531–40. **Acknowledgments** This work was supported by NIH R01 HL092055